Test Results of a Superconducting Quadrupole Model Designed for Linear Accelerator Applications

Vladimir S. Kashikhin, Nikolai Andreev, Guram Chlachidze, Joseph DiMarco, Vadim V. Kashikhin, Michael J. Lamm, Mauricio L. Lopes, Darryl Orris, Michael Tartaglia, John C. Tompkins, Gueorgui Velev, Alexander V. Zlobin

Abstract— The first model of a superconducting quadrupole for use in a Linear Accelerator was designed, built and tested at Fermilab. The quadrupole has a 78 mm aperture, and a cold mass length of 680 mm. A superferric magnet configuration with iron poles and four racetrack coils was chosen based on magnet performance, cost, and reliability considerations. Each coil is wound using enamel insulated, 0.5 mm diameter, NbTi superconductor. The quadrupole package also includes racetrack type dipole steering coils. The results of the quadrupole design, manufacturing and test, are presented. Specific issues related to the quadrupole magnetic center stability, superconductor magnetization and mechanical stability are discussed. The magnet quench performance and results of magnetic measurements will also be briefly discussed.

***Index Terms*— Linear Accelerators, Magnets, Manufacturing, Superconducting Quadrupole, Measurements, Test**

I. INTRODUCTION

A Superconducting Quadrupole intended for use in future Linear Accelerators [1-2] is now under design [3] and testing at Fermilab. Several superconducting quadrupole magnet models with similar parameters [4]-[6] have been designed and built for the LHC, the TESLA Test Facility, and XFEL. The main direction of this activity was to choose a magnetic configuration, and a magnet manufacturing technology which reached the required field integrated gradient and stability requirements.

This paper describes the magnet fabrication, test results and performance issues: the quadrupole magnetic center stability, effects caused by superconductor magnetization, and coupling effects between the quadrupole and the dipole correctors during Beam Based Alignment (BBA) procedures. Some of these issues were investigated for LHC correctors [7]-[8] but for Linear Accelerator quadrupoles, the requirement on the magnetic center stability is an order of magnitude more stringent.

Manuscript received August 17, 2007. This work was supported by the U.S. Department of Energy.

V. S. Kashikhin, N. Andreev, G. Chlachidze, J. DiMarco, V. V. Kashikhin, M. J. Lamm, M. L. Lopes, D. Orris, M. Tartaglia, J. C. Tompkins, G. Velev, A. V. Zlobin are with the Fermi National Accelerator Laboratory, Batavia, IL 60510 USA (corresponding author phone: 630-840-2899; fax: 630-840-3369; e-mail: kash@fnal.gov).

Magnetic measurements must extract the dipole field component to very high accuracy to determine the magnetic center displacement. Two methods for magnetic field measurements were used: a rotating coil system and a flat "PC-board" technique.

II. QUADRUPOLE PARAMETERS

The quadrupole model parameters chosen were close to those specified for the ILC [3] shown in Table I.

TABLE I QUADRUPOLE SPECIFICATION

Parameter	Unit	Value
Integrated peak gradient	T	36
Aperture	mm	78
Effective length	mm	660
Peak gradient	T/m	54
Field non-linearity at 5 mm radius	%	0.05
Dipole trim coils integrated strength	T-m	0.075
Quadrupole strength adjustment for BBA	%	-20
Magnetic center stability at BBA	μm	5
Magnetic center offset in cryomodule	mm	0.3
Quadrupole azimuthal offset in cryomodule	mrad	0.3
Liquid helium temperature	K	2.2
Quantity required		560

III. QUADRUPOLE POSSIBLE PROBLEMS

The main difference between quadrupole magnets used in Linear Accelerators and other accelerator magnets is a stringent requirement on magnet center stability during operation and BBA procedure. It is very difficult to provide micrometer level stability of the quadrupole magnetic center during real machine operation. This problem was investigated and good results were reported for Next Linear Collider (NLC) room temperature and adjustable permanent magnet quadrupoles [9]. It was assumed that the magnet was mounted on a sophisticated girder to compensate for center motion due to temperature changes, vibration, ground motion, etc. For Superconducting Linacs the specification for the center motion is more relaxed: 5 μm instead of 1 μm required for NLC. But

there is very limited access to a magnet mounted inside a cryostat and all center shift corrections (See Table I) should be corrected by dipole 'steering' correctors.

Factors which influence the magnetic center stability and alignment include:

- magnet misalignment;
- superconductor magnetization effects;
- ferromagnetic core saturation and hysteresis effects;
- Lorentz forces;
- external magnetic fields;
- cool down to 1.9 K and thermal deformations;
- magnet mechanical deformations;
- coupling effects between the quadrupole and dipole coils;
- magnet support structure creep;
- vibration from external sources;
- ground motion.

The influence of mechanical misalignments and magnetic effects were simulated. It was shown that these effects could cause a quadrupole center shift in the range of several tens of micrometers. So, in any scenario the dipole correctors fields are needed to compensate all magnetic center instability effects during the BBA procedure.

This conclusion drives the magnet design and performance to the following:

- The magnetic center of quadrupole must be reproducible during BBA with an accuracy of 5 μm;
- Dipole correctors should be programmed in such a way to compensate all magnetic center deviations during BBA.

The main goal of building this model magnet is to investigate the magnet cold mass magnetic center motion. The quadrupole was tested in Fermilab's Vertical Magnet Test Facility (VMTF) cryostat.

IV. Quadrupole Model Design

In general there are two options for the magnet design. The first is a shell type design [6]-[8] and the second is a "superferric" design [3], [5] where saturated iron poles form a substantial part of magnetic field in the quadrupole aperture. The second version was chosen as more promising for magnetic center stability, ease of manufacturing and lower cost. Fig. 1 and Table II show the quadrupole cross-section view and model parameters, respectively.

The proposed quadrupole has a simple configuration where the magnetic field is generated by four racetrack type coils. Field quality is not a significant issue for this magnet because the required good field region extends only to a 5 mm radius so that the positions of the iron poles and coils have relatively small influence. The iron poles, even when saturated, increase the quadrupole strength. The magnet cross-section was optimized and results were presented in [3].

The quadrupole is mounted close to the Superconducting RF Cavities (SCRF). Magnetic fields adjacent to an SCRF area must be less than 1 μT during cavity cool down to avoid trapping flux in the Nb superconductor and lower than 10 μT during cavity operation [2]. The fringe field from the quadrupole is reduced by iron end plates. The magnetic field outside the quadrupole decays from 240 gauss to less than 1 gauss at distance of 60 mm from the magnet end. It is assumed that the SCRF will have a ferromagnetic shield with efficient shielding of external fields of up to several gauss.

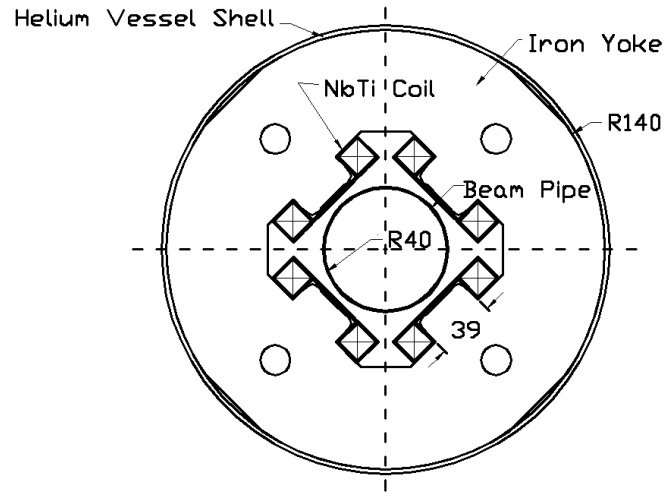

Fig. 1. Quadrupole cross-section.

TABLE II Quadrupole Model Parameters

Parameter	Unit	Value
Peak operating quadrupole and dipole current	A	100
Magnet total length	mm	680
SC wire diameter	mm	0.5
NbTi filament size (vendor value)	μm	3.7
Cu:SC volume ratio		1.5
Superconductor critical current at 5 T and 4.2 K	A	200
Coil maximum field	T	3.3
Magnetic field stored energy	kJ	40
Quadrupole inductance at 12 Hz and 20 ºC	H	3.9
Quadrupole coil number of turns/pole		700
Dipole corrector coil number of turns/pole		100
Yoke outer diameter	mm	280

V. Quadrupole Fabrication

Several technical design decisions were chosen to simplify magnet manufacturing:

- Superferric magnet configuration;
- Racetrack coils;
- Single wire winding technique;
- Coils are wound into stainless steel channels which are used as winding mandrels and as closed molds for epoxy vacuum impregnation;
- Laminated iron yoke with a single lamination used for cross-section (i.e., not four pieces);
- Coils are assembled with yoke through the magnet aperture and welded to the yoke only at the ends for an easy model disassembly.

During coil winding, high pressure accumulates on the kapton ground insulation at small radii in the coil ends. The ground insulation in these areas was substantially increased to avoid insulation breaks and corresponding shorts to the ground. The iron yoke is assembled from laser cut laminations: AISI 1006 low carbon steel of 1.5 mm thickness is being used. The overall accuracy of the measured laminations is in the range of 50 µm ; in the pole tip areas, it is 25 µm. Ferromagnetic shields were bolted at both magnet ends to reduce fringe fields. The final magnet assembly with end shields and coil connectors is shown in Fig. 10.

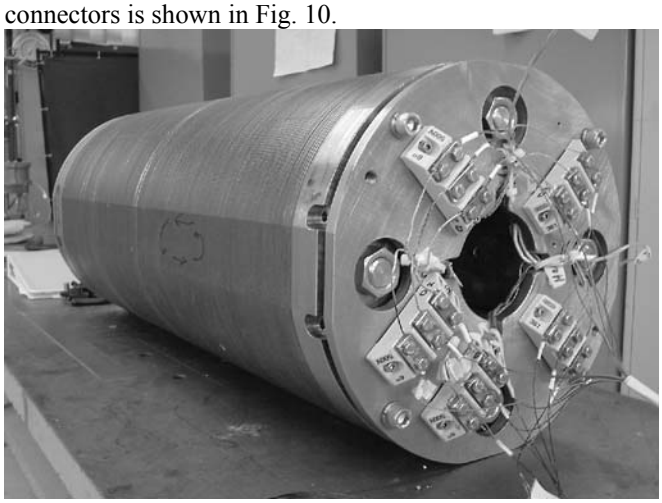

Fig. 2. Quadrupole cold mass assembly.

VI. Quadrupole Test

The VMTF test system was upgraded to perform the quadrupole package tests. Two pair of 500 A current leads were installed, and two new 300 A power supplies (PS) with a new control system were added. Due to the large magnet inductance, all ramping was done with very slow rates of current rise ('ramp rate'): a typical rate was about 0.1 A/s, the fastest was about 0.4 A/s. Actual quenches were all detected by the half-coil voltage difference (many trips occurred due to the whole coil voltage being too large when attempts to ramp too quickly occurred, such as when using the interactive PS control, instead of pre-programmed ramp profiles.) The quench history is shown in Fig. 3 with two quenches at 2 K.

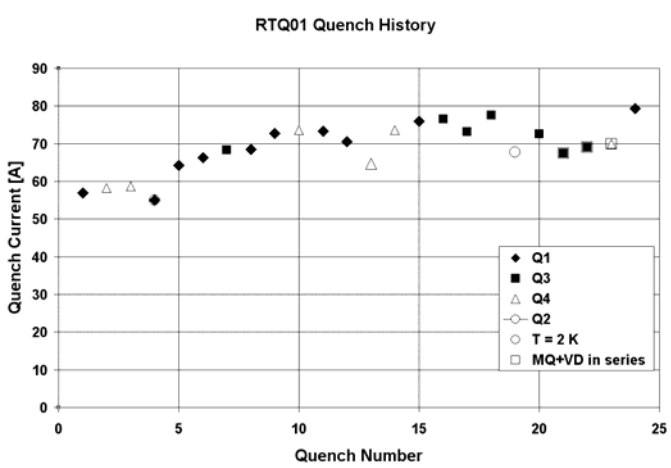

Fig. 3. Quench history and quench locations at 4.5 K and 2.2 K for RTQ01.

Note that in some cases one, or both, dipoles were connected in series with the main quadrupole (MQ+VD); thus, the peak field on the coils was greater in these cases. One could see relatively fast (36% current increase) coil training; the number of quenches per coil: Q1 – 9, Q2 – 2, Q3 – 8, and Q4 – 5. The magnet reached 80 A current and training will be continued during second test to reach the peak operating current 100 A. The voltage tap signals for all quenches show many sharp spikes distributed throughout the 1 second of data captured before the quench, and practically all quenches start with a spike (although some are very small); an example is shown in Fig. 4: each positive-going spike is accompanied by negative-going (induced) voltage spikes from the other coils. This suggests a mechanical origin for the quenches.

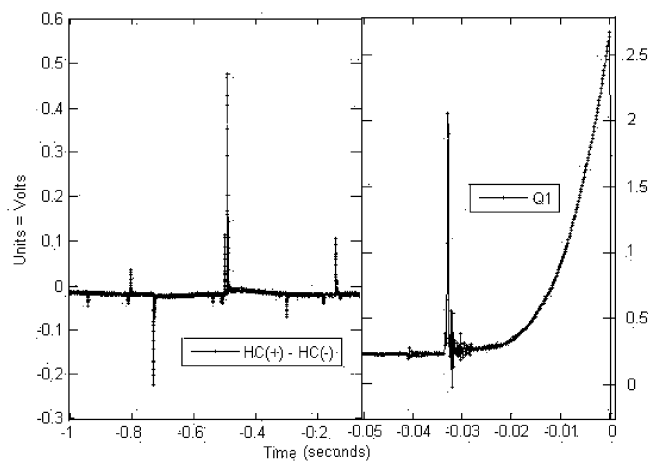

Fig. 4. Typical Quench Event (quench number 24, at 79.3 A) showing voltage spikes in various coils.

VII. Field Measurements by Rotational Coils

The well known field measurement method by rotational coils was used for the quadrupole model measurements. The basic idea of the proposed approach is to collect data from many measurements of the magnet center position with maximum achievable accuracy (in our case in order of 12 µm per measurement) for a period of time (~ 200 sec). If the center positions are distributed in a Gaussian manner, the mean value of the N measurements is determined to an accuracy of $\sigma/\sqrt{N}$, where σ is the sigma of the Gaussian distribution.

This method exploits standard rotating coil measurement technology [10]. The magnetic measurements were performed at VMTF following the quench testing. The measurements were taken at the temperatures 4.5 K. The field harmonics were measured with a rotating coil system that is integrated with a probe translation system. The translation system has the ability to position the measurement probe center in the longitudinal direction with a reproducibility of better than ±0.2 mm. A detailed description of the system can be found in [11].

The DAQ system is based on digital signal processor boards. It can continuously take data with the only limitation coming from the probe rotational speed. In the case of these measurements, the probe speed was set to 1 Hz. The average duration of a measurement was set to 200 s. Additional details on the design and operational specifications of the DAQ

system are reported in [12].

The rotational probe used for these measurements is typical of the 'tangential' style. It consists of a tangential winding, sensitive to harmonics of all orders, and two dipole and two quadrupole windings for the determination of the lowest order components of the field. The signals from the dipole and quadrupole windings provided first order information for the determination of the quadrupole center. The coil sensitivities were selected in such a way that the large dipole and quadrupole signals from the tangential winding would be naturally bucked when combined with those of the dipole and quadrupole windings. The probe radius is 20 mm and the probe is constrained by an insulating 'warm bore tube' inserted through the magnet aperture in the test dewar to provide sufficient accuracy for measurement at a 5 mm reference radius. The effective length of the probe is 81 cm providing approximately 99 % coverage of the integral field of RTQ01.

The measured field is expressed in terms of harmonic coefficients defined in a series expansion given by

$$B_y + iB_x = \sum_{n=1}^{\infty} (B_n + iA_n) \left(\frac{x+iy}{r_0} \right)^{n-1} \qquad (1)$$

where B_x and B_y in (1) are the field components in the Cartesian coordinates, B_n and A_n are the 2n-pole normal and skew field components at the reference radius r_0. The right-handed measurement coordinate system is defined with the z-axis at the center of the magnet aperture and pointing from return to lead end.

The determination of the quadrupole magnet center relative to the probe position was done using the standard technique of zeroing the dipole component assuming that it is purely generated from a probe offset. In this calculation, the "feed-down" from field harmonics three levels up is included. As a result, the quadrupole center coordinates, x_{cen} and y_{cen} were obtained. Additional details on the centering procedure were reported in [12]. The distribution of the distance R_{cen} ($R_{cen} = \sqrt{(x_{cen} \oplus y_{cen})}$) between the probe axis and magnetic center of the quadrupole for approximately N = 200 consecutive measurements is shown in Fig. 5.

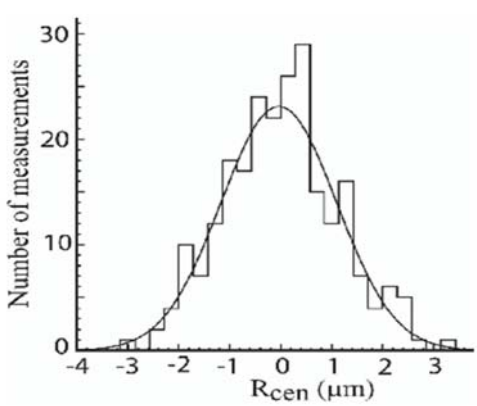

Fig. 5. Distribution of the distance R_{cen} between the probe axis and the quadrupole center of the magnet for approximately 200 measurements.

One can conclude that the distribution is well described by a Gaussian (Gaussian fit returns $\chi^2/\text{ndf} \approx 1$, solid line) with sigma of $\sigma = 1.2$ μm, which is consistent with the assumption of mechanical vibrations of the rotational system. Taking into account the number of measurements, the accuracy of determining the mean value of the distribution is given by $\sigma/\sqrt{(N)} \sim 0.1$ μm. This estimation could be affected by systematic uncertainties not yet determined. One could cancel these uncertainties by taking the difference ΔR_{cen} between two sets of measurements.

The first sets of measurements were performed when the magnet was powered to 10 A. Fig. 6 shows the results of the quadrupole center displacement ($\Delta R_{cen}(I) = R_{cen}(I) - R_{cen}(10A)$) versus magnet current (during a 'stair step' ramp up and down) where R_{cen} of the 10 A measurement was subtracted from the other currents. One might conclude that the magnet center motion is within the limits of ±2.5 μm when the current is between 3 and 10 A.

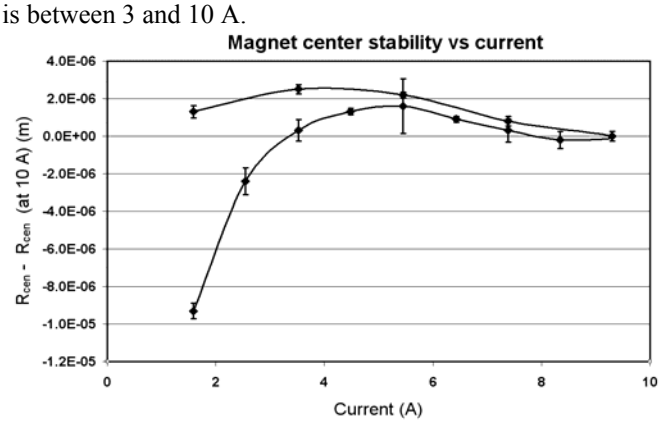

Fig. 6. $\Delta R_{cen}(I) = R_{cen}(I) - R_{cen}(10A)$. The magnet shows good center stability versus the current.

In the next set of measurements, we increased the operational current, covering the region of 10-40 A. The result is shown in Fig. 7. Unexpectedly, the quadrupole center moved linearly with a derivative of 4 μm/A of quadrupole current. This corresponds to 8 μm at 10 A and 32 μm at 40 A due the 20% current change during BBA. This effect will be investigated during next tests and may be caused by probe or quadrupole coil offsets, or an unequal number of turns in the quadrupole coils.

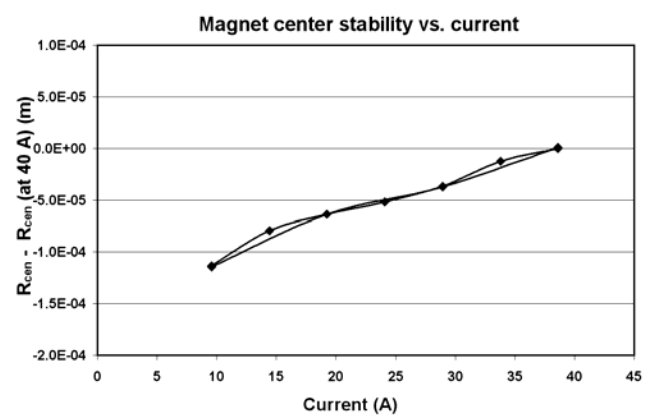

Fig. 7. ΔR_{cen} versus current. The magnetic center shows relatively large movement of ~ 100 μm during current ramp up and down.

The quadrupole is assembled with two built-in dipole

correctors: horizontal and vertical. Utilizing these two correctors, one could compensate for the linear dependence shown in Fig. 7. After subtracting this correction, the variation of quadrupole center is in the limits of ~10 μm and it is shown in Fig. 8.

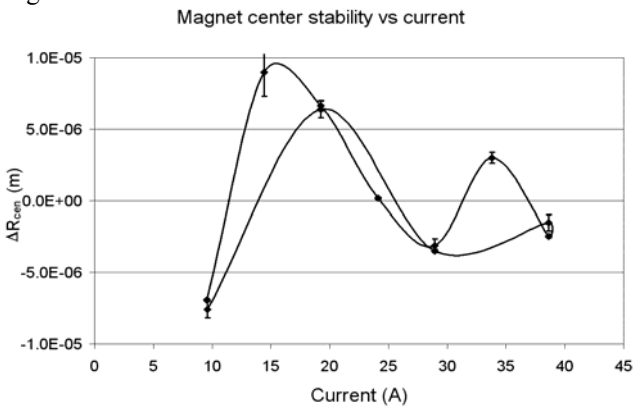

Fig. 8. ΔR_{cen} versus current. The points are corrected for the linear dependence presented at Fig. 7.

VIII. Field Measurements by a Fixed Probe

A first attempt was made to measure the stability of the quadrupole center by developing a fixed centering probe (FCP) to measure flux changes during ramping of the magnet current. The probe is 0.7 m long and was fabricated on a printed circuit board with 1200 turns over 28 layers. Most layers have a spiraling pattern of traces forming simple rectangular loops. These loops are sensitive to the dipole fields present when their axis is not coincident to the quadrupole axis; they total 1152 turns on 24 layers (48 turns per layer). Nested between these layers are 4 layers having two rectangular, adjacent loops of opposite polarity. To the extent that the loops are identical, they will buck dipole fields, but are fully sensitive to the quadrupole field. The two loops each have 12 turns for a total of 48 turns over the nested layers. A photo of the probe is shown in Fig. 9. The total trace length on the board is over 1700 m.

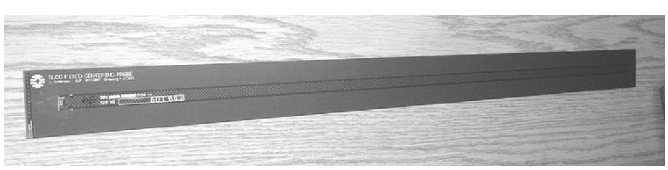

Fig. 9. The Fixed Centering Probe circuit board.

During quadrupole ramping, the change in the magnetic flux seen by the dipole bucked winding can be expressed as

$$\Delta\phi^Q = \Delta I \cdot g_{TF} \cdot R \cdot K_2^{\ Q} \qquad (1)$$

where ΔI is the change in current, g_{TF} is the gradient transfer function in T/m/A, R is the reference radius for the field measurement and K_2^Q is the n=2 (i.e. quadrupole) sensitivity of the quadrupole winding. The winding sensitivity, represented by K_n, is defined as the sum over all N wires on the probe

$$K_n = \sum_{j=1}^{N} \frac{L_j R}{n} \left(\frac{(x_j + iy_j)}{R} \right)^n (-1)^j \qquad (2)$$

Here L is the length of a given wire and R is the reference radius. The $(-1)^j$ gives the sign of the current flow of each wire and the (x_j,y_j) are the locations of the wires with respect to the probe axis. The above parameters for each wire on the probe are listed in a standard coil parameter file, and K_n calculation is straightforward.

Similarly, the change in the magnetic flux seen by the dipole sensitive (quadrupole bucked) winding can be expressed as

$$\Delta\phi^D = (\Delta I \cdot g_{TF} \cdot R) \cdot \frac{\delta}{R} \cdot K_1^{\ D} \qquad (3)$$

where δ is the offset of the probe in the quadrupole field and K_1^D is the n=1 (i.e. dipole) sensitivity of the dipole winding.

Solving equations (1) and (3) for the probe offset yields

$$\delta = \frac{\Delta\phi^D}{\Delta\phi^Q} \cdot \left(R \cdot \frac{K_2^{\ Q}}{K_1^{\ D}} \right) \qquad (4)$$

The quantity in (4) in parenthesis is a constant for the probe, (K_1^D ~22 m^2, K_2^Q is ~0.5 m^2, at R =0.0254 m).

Flux changes were measured at various DC current levels by ramping the magnet to those levels, and then starting saw-tooth current cycles of amplitude 1 A. With the large inductance 3.9 H of the magnet, power supply ramping was slow, limited to about 0.5 A/s. In order to avoid tripping the quench detection system, smooth starts/stops on the ramping were necessary, and together with about one second flattop dwell times, a single saw-tooth cycle took about 12 seconds. A data set was comprised of two saw-tooth cycles. Note that the probe angle was adjusted at the beginning of testing to read a strong (normal) quadrupole, but was not re-oriented to read in the orthogonal plane.

Data acquisition and control is run from a LabView based GUI. A user definable set of current profiles played through an NI PXI-6673 8-channel, 16-bit DAC generates the waveforms used to excite the magnet power supplies. Because of the long data acquisition times, the non-linear voltage drifts of the electronics can be large over the course of a data set. Close examination of the offset calculated from the flux ratio (See Fig. 10) shows that it additionally contains a periodic signal of amplitude ~5 microns and frequency 4-5Hz.

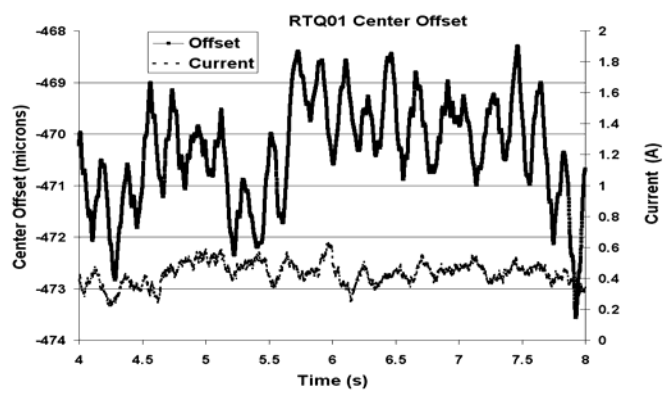

Fig. 10. Center offset calculated from raw signals.

This is thought to be caused by ground vibrations from the nearby central helium liquefier plant; these periodic vibrations

have been observed previously in the building.

To mitigate non-linear drifting with time, the offset is calculated from local flux change measurements during the ramp. The data over 0.2 s during the up-ramp and down-ramp of each cycle is extracted and fit with a second order polynomial. The change calculated from the fit for the dipole and quadrupole windings are used to calculate the offset.

Tests were run to determine the stability of the quadrupole center with no dipole corrector, dipole corrector in series with the quadrupole, and dipole corrector at various currents with a fixed quadrupole current. Data shown are from the low current studies (I < 10 A): data were taken up to 55A, but are still being evaluated.

The center stability for quadrupole only data is shown in Fig. 11. The data seem to show some shifts at the level of 10 microns, but the error bars are also at about this level for the higher currents.

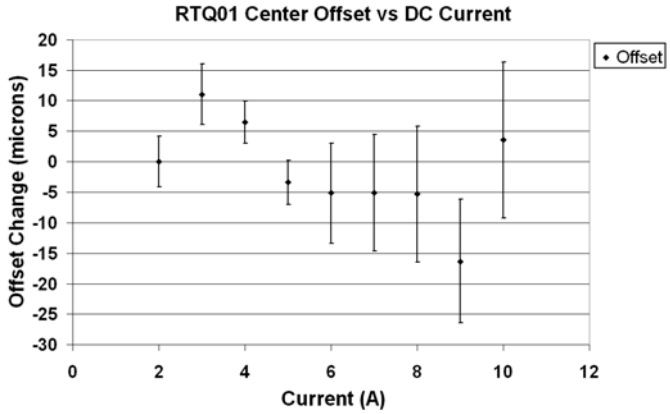

Fig. 11. Center stability for quadrupole powering only.

With the vertical dipole corrector powered in series with the quad, the center stability is shown in Fig. 12. Note that the dipole can add a very large offset to the quad but due to the series powering, it changes proportionally.

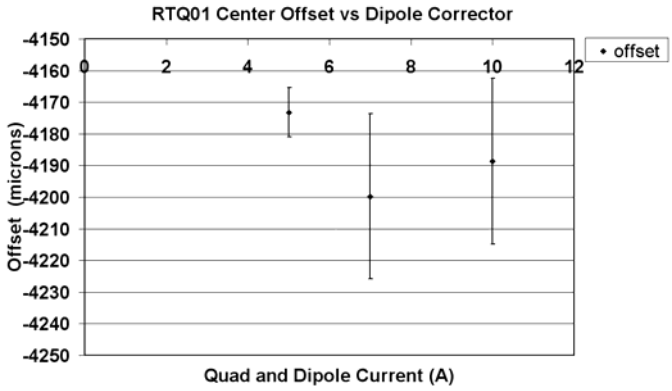

Fig. 12. Center stability with quad and dipole correctors powered in series.

With the FCP, center offset resolution appears to be on the order of 5-20 microns. Power supplies having more stability and faster ramp rate would likely improve signal size and resolution. Future tests will also better support the probe in the magnet, which was simply suspended in the beam pipe for these tests, and this may reduce some mechanical noise.

IX. Conclusion

The first Fermilab Superconducting Quadrupole for Linear Accelerators was built and tested. The test results show:

- Measured magnetic center shift ±2.5 μm at currents 3 A - 10 A;
- Probe offsets have a substantial influence on the results;
- Two different magnetic center shift measurement methods, rotating coils and a fixed centering probe, showed promising accuracy.
- It is useful to power the dipole and quadrupole coils in series for investigation of coupling effects and elimination of current imbalance;
- Due to the very large number of turns and various combinations of Lorenz forces between the quadrupole and dipole coils, the magnet needs substantial training;
- In any scenario of the BBA procedure, programmed dipole correctors must be used to compensate magnet offsets, magnet manufacturing imperfections, and various coupling effects.

A second test is planned in 2009 to continue magnet training and measurements at higher currents with upgraded measurement and test stand equipment to improve the setup and measurement accuracy.

References

[1] "International Linear Collider Reference Design Report", http://www.linearcollider.org/cms/?pid=1000025.

[2] "TESLA Design Report", Hamburg, DESY 2001-11, 2001.

[3] V. S. Kashikhin *et al.*, "Design and Manufacturing Main Linac Superconducting Quadrupole for ILC at FERMILAB", *IEEE Transactions on Applied Superconductivity*, vol. 18, No. 2, June 2008, pp. 155-158.

[4] A. Ijspeert *et al.*, "Principles developed for the construction of the high performance, low-cost superconducting LHC corrector magnets", *IEEE Transactions on Applied Superconductivity,* vol. 12, No. 1, March 2002, pp. 90-93.

[5] A. Koski, R. Bandelmann, S. Wolff, "Superconducting magnet package for the TESLA test facility", *IEEE Transactions on Magnetics*, vol. 32, No. 4, July 1996, pp. 2155-2158.

[6] F. Toral *et al.*, "Design and fabrication study on the TESLA500 superconducting magnets", *IEEE Transactions on Applied Superconductivity*, vol. 12, No. 1, March 2002, pp. 282-286.

[7] W. Venturini Delsorado, M. Karppinen, "Cold test results of the inner triplet orbit correctors for the LHC", *IEEE Transactions on Applied Superconductivity*, vol. 16, No. 2, June 2006, pp. 277-280.

[8] L. Bottura *et al.*, "Magnetic alignment measurements at room and cryogenic temperature of LHC cryodipoles and associated correctors at CERN", *IEEE Transactions on Applied Superconductivity*, vol. 14, No. 2, June 2004, pp. 227-230.

[9] J. T. Volk *et al.,* "Adjustable Permanent Quadrupoles for the Next Linear Collider", *Proceedings of the 2001 Particle Accelerator Conference*, Chicago, pp. 218–219.

[10] A. Jain, "Harmonic coils", CERN 98-05, Aug. 1998.

[11] N. Andreev *et al.*, "Field quality in Fermilab-built models of high gradient quadrupole magnets for the LHC interaction region", *IEEE Trans. Appl. Supercond.*, Vol. 10, 2000, pp. 107-110

[12] G.V. Velev *et al.,* "A Fast Continuous Magnetic Field Measurement System Based on Digital Signal Processors", IEEE Trans. of Applied Superconductivity, Vol. 16, No. 2, June 2006, pp. 1374-1377.